

# All Polyhedral Manifolds are Connected by a 2-Step Refolding

Lily Chung\*    Erik D. Demaine\*    Jenny Diomidova\*    Tonan Kamata†  
 Jayson Lynch\*    Ryuhei Uehara†    Hanyu Alice Zhang‡

## Abstract

We prove that, for any two polyhedral manifolds  $\mathcal{P}, \mathcal{Q}$ , there is a polyhedral manifold  $\mathcal{I}$  such that  $\mathcal{P}, \mathcal{I}$  share a common unfolding and  $\mathcal{I}, \mathcal{Q}$  share a common unfolding. In other words, we can unfold  $\mathcal{P}$ , refold (glue) that unfolding into  $\mathcal{I}$ , unfold  $\mathcal{I}$ , and then refold into  $\mathcal{Q}$ . Furthermore, if  $\mathcal{P}, \mathcal{Q}$  are embedded in 3D, then  $\mathcal{I}$  can be embedded in 3D (without self-intersection). These results generalize to  $n$  given manifolds  $\mathcal{P}_1, \mathcal{P}_2, \dots, \mathcal{P}_n$ ; they all have a common unfolding with an intermediate manifold  $\mathcal{I}$ . Allowing more than two unfold/refold steps, we obtain stronger results for two special cases: for doubly covered convex planar polygons, we achieve that all intermediate polyhedra are planar; and for tree-shaped polycubes, we achieve that all intermediate polyhedra are tree-shaped polycubes.

## 1 Introduction

Consider a *polyhedral manifold* — a connected two-dimensional surface made from flat polygons by gluing together paired portions of boundary (but possibly still leaving some boundary unpaired, and not necessarily embedded in space without overlap). Two basic operations on such a manifold are *gluing* (joining together two equal-length portions of remaining boundary) and the inverse operation *cutting* (splitting a curve into two equal-length portions of boundary, while preserving overall connectivity of the manifold). If we cut a manifold  $\mathcal{P}$  enough that it can be laid isometrically into the plane (possibly with overlap), we call the resulting flat shape  $U$  an *unfolding* of  $\mathcal{P}$ .<sup>1</sup> Conversely, if we glue a flat shape  $U$  into any polyhedral manifold  $\mathcal{P}$ , we call  $\mathcal{P}$  a *folding* of  $U$  (and  $U$  an unfolding of  $\mathcal{P}$ ).

(Un)foldings naturally define an infinite bipartite graph  $\mathbf{G}$  [DO07, Section 25.8.3]: define a vertex on one side for each manifold  $\mathcal{P}$ , a vertex on the other side for each flat shape  $U$ , and an edge between  $U$  and  $\mathcal{P}$  whenever  $U$  is an unfolding of  $\mathcal{P}$  (or equivalently,  $\mathcal{P}$  is a folding of  $U$ ). Because unfolding and folding preserve surface area, we can naturally restrict the graph to manifolds and flat shapes of a fixed surface area  $A$ . Is the resulting graph  $\mathbf{G}_A$  connected? In other words, is it possible to transform any polyhedral manifold into any other polyhedral manifold of the same surface area by an alternating sequence of unfolding to a flat shape, folding that flat shape into a new manifold, unfolding that manifold into a flat shape, and so on? We call each pair of steps — unfolding and then folding — a *refolding step*. We can then ask whether two manifolds have a  $k$ -step refolding for each  $k = 1, 2, \dots$ .

\*Computer Science and Artificial Intelligence Laboratory, Massachusetts Institute of Technology, USA.

†School of Information and Science, Japan Advanced Institute of Science and Technology, Japan.

‡School of Applied and Engineering Physics, Cornell University, USA.

<sup>1</sup>Note that our notion of “unfolding” differs from many other uses, such as [DO07], which forbid overlap. But it matches most previous work on refolding [DDD<sup>+</sup>23, ADKU22].

In this paper, we give the first proof that the graph  $G_A$  is connected. In fact, we show that the graph has diameter at most 2: every pair  $\mathcal{P}, \mathcal{Q}$  of polyhedral manifolds have a 2-step refolding. In other words, there is a single polyhedral manifold  $\mathcal{I}$  such that  $\mathcal{P}$  and  $\mathcal{I}$  share a common unfolding, as do  $\mathcal{I}$  and  $\mathcal{Q}$ . This result turns out to follow relatively easily using classic results from common dissection, similar in spirit to general algorithms for hinged dissection [AAC<sup>+</sup>12].

More interesting is that we show similar results when we restrict the polyhedral manifolds to the following special cases, which reduce the allowed input manifolds  $\mathcal{P}, \mathcal{Q}$ , but importantly also reduce the allowed intermediate manifolds  $\mathcal{I}$ :

1. **No boundary:** If polyhedral manifolds  $\mathcal{P}$  and  $\mathcal{Q}$  have no boundary (what we might call “polyhedra”), then there is a 2-step refolding where the intermediate manifold  $\mathcal{I}$  also has no boundary. This version is similarly easy. (In fact, we can achieve this property even when  $\mathcal{P}$  and  $\mathcal{Q}$  have boundary.)
2. **Embedded:** If polyhedral manifolds  $\mathcal{P}$  and  $\mathcal{Q}$  are embedded in 3D, then there is a 2-step refolding where the intermediate manifold  $\mathcal{I}$  is embedded in 3D. Furthermore, if  $\mathcal{P}$  and  $\mathcal{Q}$  have no boundary, then  $\mathcal{I}$  also has no boundary. This result is our main technical achievement.
3. **Doubly covered convex polygons:** If polyhedral manifolds  $\mathcal{P}$  and  $\mathcal{Q}$  are doubly covered convex polygons, then there is an  $O(n)$ -step refolding where every intermediate manifold  $\mathcal{I}$  is “planar” (all polygons lie in the plane, but possibly with multiple layers) and has no boundary. This result follows from an  $O(1)$ -step refolding to remove a vertex from a doubly covered convex polygon.
4. **Polycubes:** If polyhedral manifolds  $\mathcal{P}$  and  $\mathcal{Q}$  are the surfaces of tree-shaped  $n$ -cubes (made from  $n$  unit cubes joined face-to-face according to a tree dual), then there is an  $O(n^2)$ -step refolding where every intermediate manifold  $\mathcal{I}$  is a (possibly self-intersecting) tree-shaped  $n$ -cube. Furthermore, the refoldings involve cuts only along edges of the cubes (*grid edges*); and if the given polycubes do not self-intersect and are “well-separated”, then the intermediate polycubes also do not self-intersect. This result follows from simulating operations in reconfigurable robots.

Past work on refolding has focused on the restriction to polyhedral manifolds that are the surfaces of *convex polyhedra*. This version began with a specific still-open question — is there a 1-step refolding from a cube to a regular tetrahedron? — independently posed by M. Demaine (1998), F. Hurtado (2000), and E. Pegg (2000). When E. Demaine and J. O’Rourke wrote this problem in their book [DO07, Open Problem 25.6], they also introduced the multi-step refolding problem. Let  $C_A$  be the subgraph of  $G_A$  restricting to convex polyhedra and their unfoldings. Demaine, Demaine, Diomidova, Kamata, Uehara, and Zhang [DDD<sup>+</sup>23] showed that several convex polyhedra of surface area  $A$  are all in the same connected component of  $C_A$ : doubly covered triangles, doubly covered regular polygons, tetramonohedra (tetrahedra whose four faces are congruent acute triangles, including doubly covered rectangles), regular prisms, regular prisms, regular prisms, augmented regular prisms, and all five Platonic solids. These refoldings require just  $O(1)$  steps (at most 9).

Our 2-step refolding is very general, applying in particular to any two convex polyhedra, but crucially relies on a nonconvex intermediate manifold  $\mathcal{I}$ . We conjecture that two steps is also optimal, even for two convex polyhedra. Indeed, Arseneva, Demaine, Kamata, and Uehara [ADKU22] conjectured that most pairs of doubly covered triangles (specifically, those with rationally independent angles) have no common unfolding, and thus no 1-step refolding. As evidence, they showed (by exhaustive search) that any common unfolding has at least 300 vertices. Assuming this conjecture, two steps are sometimes necessary. Two steps is also the first situation where we

have an intermediate manifold  $\mathcal{I}$ , which is what allows us to exploit the additional freedom of the nonconvexity of  $\mathcal{I}$ .

We use the simpler cases of doubly covered convex polygons (Section 3) and polycubes (Section 4) as warmups for our general 2-step refolding (Section 5).

## 2 Refolding Model

In our constructions, we use a more general but equivalent form of “refolding step”: any cutting followed by any gluing. In other words, we allow using an arbitrary connected manifold in between cutting and gluing. By contrast, the definition in Section 1 requires a full unfolding followed by a folding, which requires a flat shape in between cutting and gluing.

These two models are equivalent. If we want to modify one of our refolding steps to instead reach a full unfolding after cutting, we can perform additional cuts (that preserve connectivity) until the manifold can be laid flat, and then immediately reglue those cuts back together. The same idea is used in [DDD<sup>+</sup>23].

## 3 Transformation Between Doubly Covered Convex Polygons

We start with *doubly covered convex polygons*, that is, polyhedral manifolds without boundary formed from two copies of a convex planar polygon by gluing together all corresponding pairs of edges. Here we require that every intermediate polyhedral manifold  $\mathcal{I}$  is *planar* in the sense that its polygons all lie in the plane, but we allow any number of layers of stacked polygons, generalizing the notion of doubly covered polygon.

**Theorem 1.** *Any two doubly covered convex  $n$ -gons of the same area have an  $O(n)$ -step refolding, where all intermediate manifolds are planar with no boundary.*

As a useful building block, we consider a simple 2-step refolding which allows removing a piece from the polygon, rotating it, and gluing it back elsewhere (similar to hinged dissection), provided we can fold the polygon to facilitate the gluing.

**Lemma 2.** *Let  $P$  be a subset of the plane homeomorphic to a closed disk, and suppose  $\overline{A_1B_1}$  and  $\overline{A_2B_2}$  are line segments on the boundary of  $P$ , such that there exists a plane reflection  $r$  taking  $A_1$  to  $A_2$  and  $B_1$  to  $B_2$ . Let  $c$  be a simple curve starting and ending on the boundary of  $P$  passing through its interior, so that it separates  $P$  into two closed halves  $P_1$  and  $P_2$  containing  $\overline{A_1B_1}$  and  $\overline{A_2B_2}$  respectively. Let  $f$  be the unique rotation and translation such that  $f(A_1) = A_2$  and  $f(B_1) = B_2$ , and suppose  $f(P_1)$  intersects  $P_2$  only on  $\overline{A_2B_2}$ . Then there is a 2-step refolding between the double covers of  $P$  and  $P'$ , where  $P' = f(P_1) \cup P_2$ .*

*Proof.* The refolding is accomplished by the following steps, illustrated in Figure 1:

1. Cut along  $\overline{A_1B_1}$  and  $\overline{A_2B_2}$ , then glue the top layer of  $\overline{A_1B_1}$  to the top layer of  $\overline{A_2B_2}$  and similarly for the bottom layers. This intermediate step can be folded flat by a single fold along the line of reflection of  $r$ .
2. Cut along  $c$  in both layers to create two new boundaries  $c_1$  and  $c_2$ . Then glue the top layer of  $c_1$  to the bottom layer of  $c_1$  and similarly for  $c_2$ . □

Now we consider the triangle  $\triangle ABC$  formed by three consecutive vertices  $A, B, C$  on the boundary of a polygon  $P$ . Our goal is to find an  $O(1)$ -step refolding of  $P$  which moves the apex

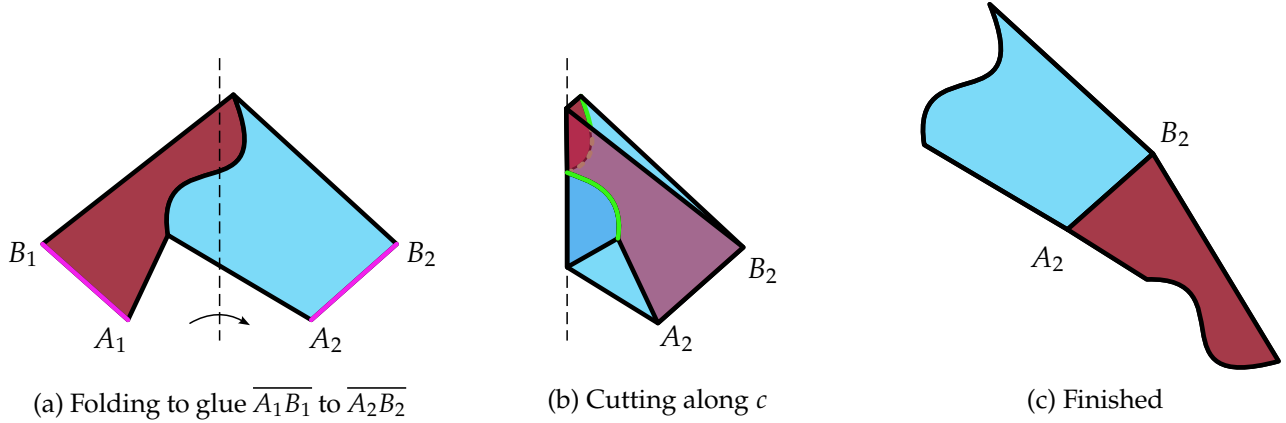


Figure 1: Rearranging two pieces via a 2-step refolding.

$B$  parallel to  $AC$  (which preserves area). This will allow us to move  $B$  so that the interior angle at  $C$  becomes  $180^\circ$ , eliminating a vertex from  $P$ . By induction, this allows us to reduce any doubly covered polygon down to a doubly covered triangle, and then we can use a known 3-step refolding between doubly covered triangles [DDD<sup>+</sup>23, Theorem 2]. We accomplish the goal as follows:

**Lemma 3.** *Let  $P$  be a convex polygon with three consecutive vertices  $A, B, C$  such that the projection of  $B$  onto  $AC$  is between  $A$  and  $C$ . Then there is an  $O(1)$ -step refolding between the double covers of  $P$  and  $P'$ , where  $P'$  is the polygon obtained from  $P$  by replacing  $\triangle ABC$  by a rectangle with base  $\overline{AC}$  with the same area.*

*Proof.* Refer to Figure 2. Let  $X$  be the midpoint of  $\overline{AB}$ ,  $Y$  be the midpoint of  $\overline{BC}$ , and  $O$  be the projection of  $B$  onto  $XY$ . Using Lemma 2, we rotate  $\triangle XBO$  by  $180^\circ$  about  $X$ , and similarly we rotate  $\triangle YBO$  by  $180^\circ$  about  $Y$ . This forms the desired rectangle.  $\square$

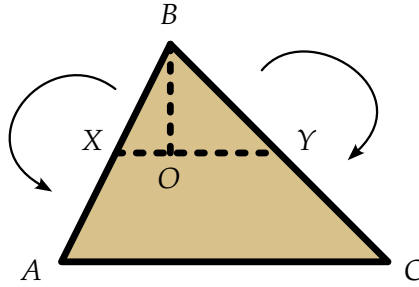


Figure 2: Refolding  $\triangle ABC$  into a rectangle when  $B$  is between  $A$  and  $C$ .

**Lemma 4.** *Let  $P$  be a convex polygon with three consecutive vertices  $A, B, C$ , and let  $B_1$  be the projection of  $B$  onto  $AC$ . Suppose that  $C$  is between  $A$  and  $B_1$ , and  $|CB_1| \leq 4|AC|$ . Then there is an  $O(1)$ -step refolding between the double covers of  $P$  and  $P'$ , where  $P'$  is the polygon obtained from  $P$  by replacing  $\triangle ABC$  by a rectangle with base  $\overline{AC}$  with the same area.*

*Proof.* Refer to Figure 3. Let  $X$  be the midpoint of  $\overline{AB}$  and  $Y$  be the midpoint of  $\overline{BC}$ . For this proof we will adopt the convention that  $p_1$  denotes the projection of  $p$  onto  $AC$  and  $p_2$  denotes the projection of  $p$  onto  $XY$ .

Using Lemma 2 we rotate  $\triangle XYB$  by  $180^\circ$  about  $X$ , forming a parallelogram  $ACY'Y'$ . Now let  $W$  be the midpoint of  $CY$  and  $V$  be the midpoint of  $AY'$ . We have

$$|AV_1| = |W_2Y| = \frac{1}{4}|CB_1| \leq |AC| = |Y'Y|,$$

which implies  $V_1$  lies on  $\overline{AC}$  and  $W_2$  lies on  $\overline{Y'Y}$ . Using Lemma 2 twice, we rotate  $\triangle AVV_1$  by  $180^\circ$  about  $V$ , and  $\triangle YWW_2$  by  $180^\circ$  about  $W$ . This forms a rectangle  $V_1W_1W_2V_2$ . Finally, we use Lemma 2 again to move the rectangle  $CW_1W_2C_2$  to  $AV_1V_2A_2$ .  $\square$

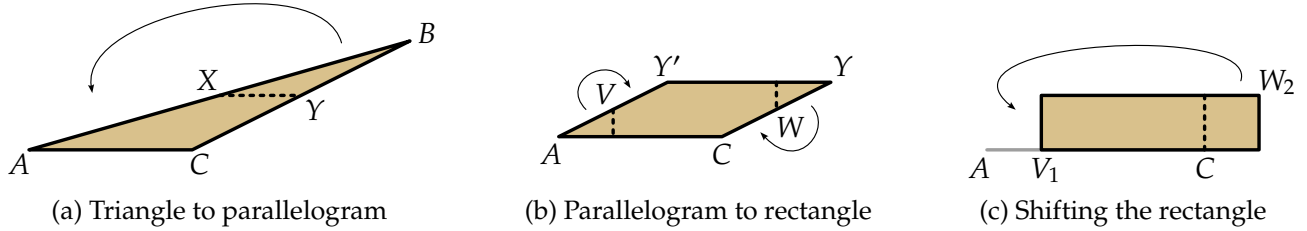


Figure 3: Refolding  $\triangle ABC$  into a rectangle when  $B$  is to the right of  $C$ .

**Lemma 5.** Let  $P$  be a convex polygon with three consecutive vertices  $A, B, C$  and let  $Z$  be another vertex of  $P$  such that the interior angle at  $Z$  is smaller than the interior angle at  $B$ . Let  $\ell$  be the line through  $B$  parallel to  $AC$ ,  $Q_1$  be the intersection of  $ZA$  with  $\ell$ , and  $Q_2$  be the intersection of  $ZC$  with  $\ell$ . Then  $\min\{|Q_1B|, |Q_2B|\} \leq |AC|$ .

*Proof.* Refer to Figure 4. Construct  $B'$  so that  $ABCB'$  is a parallelogram. Vertex  $Z$  cannot lie in the interior of  $\triangle ACB'$  or else its interior angle would be larger than that of  $B$  (by convexity of  $P$ ). Thus  $Z$  is either below  $AB'$  or below  $CB'$ ; in the first case, we have  $|Q_1B| \leq |AC|$ , and in the second case, we have  $|Q_2B| \leq |AC|$ .  $\square$

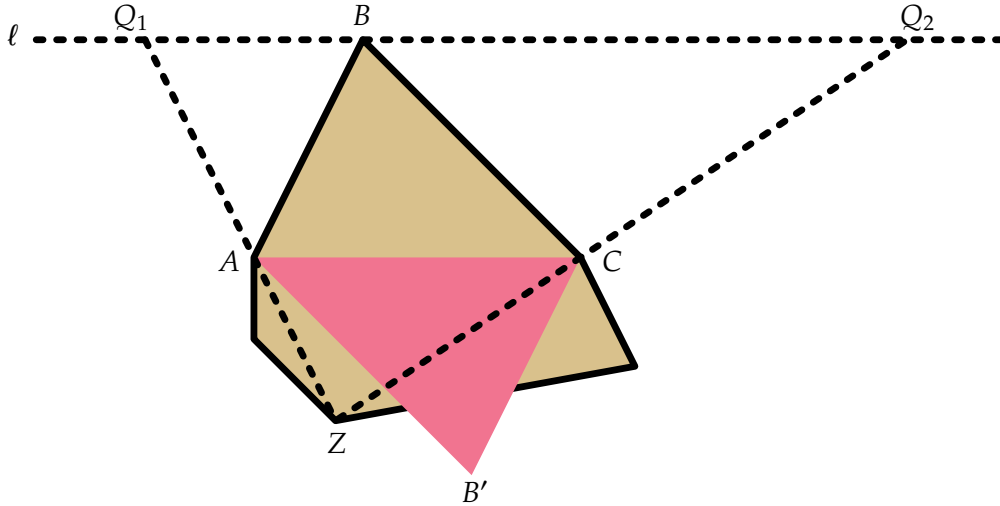


Figure 4: Bounding the distance from  $B$  to  $Q_1, Q_2$ .

**Corollary 6.** Let  $P$  be a convex polygon with five consecutive vertices  $D_1, A, B, C, D_2$  (where possibly  $D_1 = D_2$ ) such that the interior angle at  $B$  is larger than the interior angles at  $D_1$  and  $D_2$ . Let  $\ell$  be the line through  $B$  parallel to  $AC$ ,  $Q_1$  be the intersection of  $D_1A$  with  $\ell$ , and  $Q_2$  be the intersection of  $D_2C$  with  $\ell$ . Then  $\min\{|Q_1B|, |Q_2B|\} \leq |AC|$ .

*Proof.* By convexity of  $P$ ,  $D_1$  is below  $D_2A$  and so  $|Q_1B|$  is at most the distance from  $B$  to the intersection of  $D_2A$  with  $\ell$ . The inequality thus follows from Lemma 5 applied to  $D_2$ .  $\square$

*Proof of Theorem 1.* It suffices to show that, for  $n \geq 4$ , any doubly covered convex  $n$ -gon can be reduced to a doubly covered convex  $(n - 1)$ -gon by an  $O(1)$ -step refolding, because then we can reduce both polygons to triangles in  $O(n)$  steps, and [DDD<sup>+</sup>23, Theorem 2] shows there is a 3-step refolding between any pair of doubly covered triangles with the same area.

Let  $P$  be a convex  $n$ -gon where  $n \geq 4$ , and let  $B$  be a vertex of  $P$  with the largest interior angle. By Corollary 6 we can label the nearby vertices of  $B$  by  $A, C, D$  such that  $A, B, C, D$  are consecutive and  $|QB| \leq |AC|$  where  $Q$  is the intersection of  $DC$  with  $\ell$ , the line through  $B$  parallel to  $AC$ . Let  $P'$  be the polygon obtained from  $P$  by replacing  $\triangle ABC$  by a rectangle with base  $\overline{AC}$  of the same area, and let  $P''$  be the polygon obtained from  $P$  by replacing  $\triangle ABC$  by  $\triangle AQC$ . By Lemma 3, there is an  $O(1)$ -step refolding between the double covers of  $P$  and  $P'$ ; it applies because the interior angle of  $B$  is at least  $90^\circ$ . Similarly, one of Lemmas 3 or 4 (using  $|QB| \leq |AC|$ ) shows that there is an  $O(1)$ -step refolding between the double covers of  $P''$  and  $P'$ . Thus there is an  $O(1)$ -step refolding between double covers of  $P$  and  $P''$ . But because  $D, C, Q$  are collinear,  $P''$  is a convex  $(n - 1)$ -vertex polygon.  $\square$

## 4 Transformation Between Tree-Shaped Polycubes

Next we consider *tree-shaped  $n$ -cubes*, that is, polyhedral manifolds formed from  $n$  unit cubes in 3D *joined* face-to-face in a tree structure (forming a tree dual graph). Here, when two cubes get joined together at a common face, we remove that face from the manifold, preserving that the manifold is homeomorphic to a disk. (This notion of “join” is a higher-dimensional analog of gluing.) Thus every tree-shaped  $n$ -cube has surface area  $6n - 2(n - 1) = 4n + 2$ .

We allow two cubes to be adjacent even if they are not glued together, in which case there are two surface squares in between. If there are no such touching cubes, we call the tree-shaped  $n$ -cube *well-separated*. When the  $n$ -cubes are not well-separated, we further allow multiple cubes to occupy the same location in space, in which case we call the tree-shaped  $n$ -cube *self-intersecting*.

All cubes of a tree-shaped  $n$ -cube naturally lie on a cubical grid. Define *grid cutting* to be cutting restricted to edges of the cubical grid, and *grid refolding* to be grid cutting followed by gluing that results in another tree-shaped  $n$ -cube.

**Theorem 7.** *Any two tree-shaped  $n$ -cubes have an  $O(n^2)$ -step grid refolding, where all intermediate manifolds are possibly self-intersecting tree-shaped  $n$ -cubes. If the given tree-shaped  $n$ -cubes do not self-intersect and are well-separated, then the intermediate manifolds do not self-intersect.*

To transform between two given tree-shaped polycubes  $\mathcal{P}$  and  $\mathcal{Q}$ , we mimic the “sliding cubes” model of reconfiguring modular robots made up of  $n$  cubes, which was recently solved in optimal  $O(n^2)$  steps [AAK<sup>+</sup>24]. This model defines two types of operations (see Figure 5):

1. *Slide* a cube along a flat surface of neighboring cubes by 1 unit.
2. *Rotate* a cube around the edge of an adjacent cube.

We will show to perform slide and rotate operations for a *leaf* cube, that is, a leaf of the dual tree in a tree-shaped polycube. In this case, sliding can be viewed as moving a leaf cube to a new parent, and rotating can be viewed as the leaf cube attaching to a different location of the same parent.

To slide a leaf cube, we perform the following refolding step, illustrated in Figure 6:

1. Cut  $AB, BE, ED, FG, GJ$ , and  $IJ$ . These cuts free up the leaf cube to move into the adjacent location, as drawn in the intermediary figure in Figure 6.

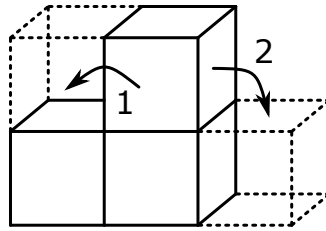


Figure 5: Two different ways an individual cube can move on a surface of a polycube: (1) sliding and (2) rotating.

2. Glue  $AB'$  to  $E'B'$ ,  $FG'$  to  $J'G'$ ,  $E'D$  to  $AB$ ,  $J'I$  to  $FG$ ,  $DE$  to  $BE$ , and  $IJ$  to  $GJ$ .

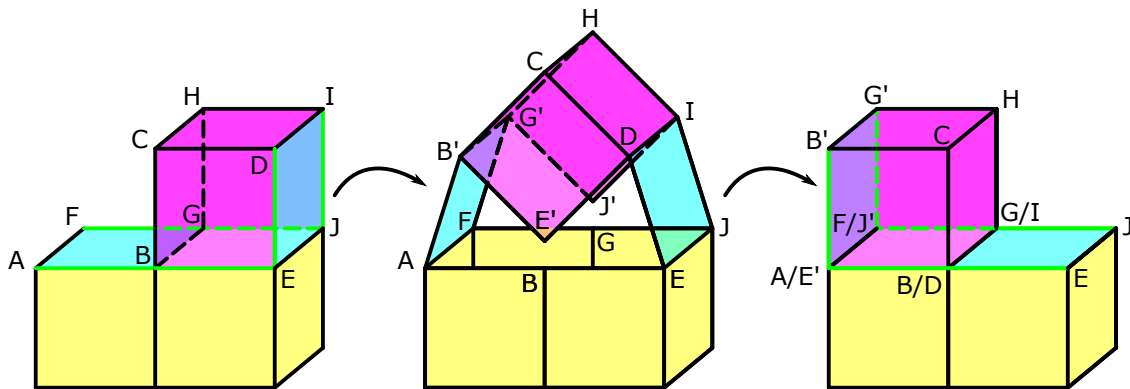


Figure 6: Sliding a leaf cube.

Figure 7 shows an extension of sliding. Here the leaf cube  $IDEJCHGB$  does not move, but it changes its parent from the cube attached below to the cube attached on its left, effectively traversing the reflex corner. The same refolding step as sliding applies in this case.

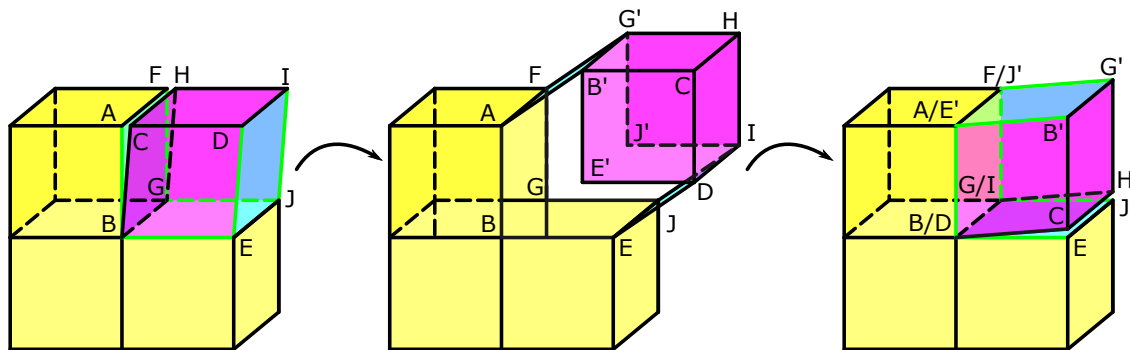


Figure 7: "Sliding" a leaf cube in a reflex corner.

To rotate a leaf cube around an edge we perform the following refolding step, illustrated in Figure 8:

1. Cut  $BA$ ,  $AD$ ,  $DE$ ,  $GF$ ,  $FI$ , and  $IJ$ . Similar to the sliding procedure, these cuts free up the leaf cube to move, as shown in the intermediary figure in Figure 8.
2. Glue  $AB$  to  $AD$ ,  $FG$  to  $FI$ ,  $BA'$  to  $DE$ ,  $GF'$  to  $IJ$ ,  $A'D'$  to  $ED'$ , and  $F'I'$  to  $JI'$ .

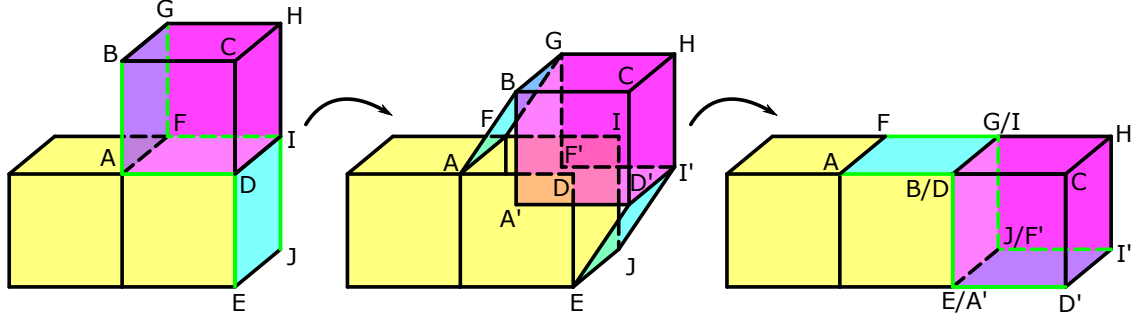


Figure 8: Rotating a leaf cube over the edge of a polycube.

By combining these three operations, we can follow a simple algorithm for transforming a given  $n$ -cube  $\mathcal{P}$  into a  $1 \times 1 \times n$  line:

1. Fix one leaf cube as the *root* cube  $c_1$ . Assume by symmetry that the root cube's unique neighbor is in the down direction.
2. For  $i = 2, 3, \dots, n$ :
  - (a) Assume  $c_1, \dots, c_{i-1}$  have been arranged into an upward line, with  $c_i$  being a current leaf.
  - (b) Take a leaf cube  $c_i$  that is not  $c_{i-1}$  (given that there are always at least two leaves).
  - (c) Slide and rotate  $c_i$  around the boundary of the rest of the tree until it reaches the root cube  $c_1$ , and then slide it up the line to place it immediately above  $c_{i-1}$ .

This algorithm requires  $O(n^2)$  steps: potentially each of the  $n$  cubes needs to traverse the surface area of the tree-shaped  $n$ -cube, which is  $O(n)$ . It may also cause self-intersection, because it blindly follows the surface of the tree-shaped  $n$ -cube, so it may place the moving leaf cube on top of an adjacent cube in the case of touching cubes. If the tree-shaped  $n$ -cube is well-separated, though, then this simple algorithm avoids self-intersection.

To transform between two tree-shaped  $n$ -cubes  $\mathcal{P}$  and  $\mathcal{Q}$ , we apply the algorithm above separately to each of  $\mathcal{P}$  and  $\mathcal{Q}$ , perform the refolding steps on  $\mathcal{P}$  to transform it into a line, and then perform the reverse refolding steps on  $\mathcal{Q}$  to transform the line into it. (Note that each refolding step is reversible.) Thus we have proved Theorem 7.

It is tempting to apply the (much more complicated)  $O(n^2)$ -step algorithm of Abel, Akitaya, Kominers, Korman, and Stock [AAK<sup>+</sup>24], which has the advantage of avoiding self-intersection without any assumption of well-separation. Unfortunately, sliding and rotating nonleaf cubes seems more difficult. One approach is to transform one spanning tree into another (probably increasing the number of steps), but it is not even clear whether this can be done by leaf reparenting operations.

It also seems likely that some of these moves can be done in parallel in the same refolding step, leading to fewer refolding steps. Some models of modular robotics have parallel reconfiguration algorithms that move a linear number of robots in each round [ACD<sup>+</sup>08, ACD<sup>+</sup>09]. It remains open whether we can get similarly good bounds in the cube sliding model or the leaf-focused sliding-by-refolding model.



## 5 Transformation Between Polyhedral Manifolds

In this section, we prove the main result of the paper:

**Theorem 8.** *Any two polyhedral manifolds  $\mathcal{P}, \mathcal{Q}$  of the same surface area have a 2-step refolding. If  $\mathcal{P}$  and  $\mathcal{Q}$  have no boundary, then so does the intermediate manifold  $\mathcal{I}$ . If  $\mathcal{P}$  and  $\mathcal{Q}$  are embedded in 3D, then so is the intermediate manifold  $\mathcal{I}$ .*

Sections 5.1–5.3 are devoted to the proof. Then Section 5.5 will generalize to  $n$  manifolds:

**Corollary 9.** *For any  $n$  polyhedral manifolds  $\mathcal{P}_1, \dots, \mathcal{P}_n$  of the same surface area, there is another polyhedral manifold  $\mathcal{I}$  such that  $\mathcal{P}_i$  and  $\mathcal{I}$  have a common unfolding for all  $i$ . If manifolds  $\mathcal{P}_i$  have no boundary, then so does  $\mathcal{I}$ . If manifolds  $\mathcal{P}_i$  are embedded in 3D, then so is  $\mathcal{I}$ .*

### 5.1 Abstract Intermediate Polyhedron

We start by proving the first two claims in Theorem 8, ignoring the requirement of embeddability of the intermediate manifold  $\mathcal{I}$ . This serves as a useful warmup and an overview of our methods.

We start by computing a *common dissection* of the given manifolds  $\mathcal{P}$  and  $\mathcal{Q}$  of equal surface area, that is, a subdivision of each surface into polygons that match in the sense that, for some perfect pairing of  $\mathcal{P}$ 's polygons with  $\mathcal{Q}$ 's polygons, there is an isometry between paired polygons. Solutions to this dissection problem go back to the early 1800s [Low14, Wal31, Bol33, Ger33]. See [AAC<sup>+</sup>12] for a more algorithmic description, and pseudopolynomial bounds on the number of pieces. We can further assume that the dissection is a triangulation, where triangles meet edge-to-edge, by triangulating each polygon in the dissection.

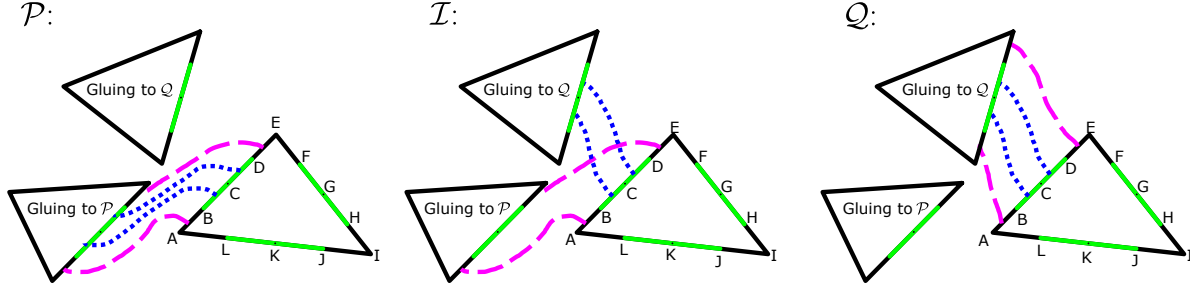


Figure 9: 2-step refolding of each triangle  $\triangle AEI$  from  $\mathcal{P}$  to  $\mathcal{Q}$ , via an abstract intermediate manifold  $\mathcal{I}$ .

Now consider an arbitrary triangle  $\triangle AEI$  in the common triangulation of  $\mathcal{P}$  and  $\mathcal{Q}$ , as shown in Figure 9. We divide each edge of this triangle  $\triangle AEI$  into four line segments of equal length:  $AE$  divides into  $AB = BC = CD = DE$ ,  $EI$  divides into  $EF = FG = GH = HI$ , and  $IA$  divides into  $IJ = JK = KL = LA$ .<sup>2</sup> The (abstract) intermediate manifold  $\mathcal{I}$  glues this triangle to other triangles using a mixture of the gluings from  $\mathcal{P}$  and  $\mathcal{Q}$ : the outer edges  $AB, DE, EF, HI, IJ$ , and  $LA$  are glued as in  $\mathcal{P}$ , while the inner edges  $BC, CD, FG, GH, JK$ , and  $KL$  are glued as in  $\mathcal{Q}$ .

In more detail, our 2-step refolding algorithm from  $\mathcal{P}$  to  $\mathcal{Q}$  works as follows:

**Cut 1:** For each triangle  $\triangle AEI$ , cut the inner edges  $BC, CD, FG, GH, JK$ , and  $KL$  (represented by blue dotted lines in Figure 9). Because no cut fully separates an entire edge from its mate in  $\mathcal{P}$ , this cutting preserves connectivity.

<sup>2</sup>For orientable surfaces, it would be enough to divide each edge into only two equal line segments, but the symmetry of four segments enables even non-orientable (flipped) gluings; it will also be useful when we make  $\mathcal{I}$  embeddable.

**Glue 1:** For each triangle  $\triangle AEI$ , glue the inner edges  $BC$ ,  $CD$ ,  $FG$ ,  $GH$ ,  $JK$ , and  $KL$  to their neighbors in  $Q$  when they exist (as in Figure 9, middle), producing the (abstract) intermediate manifold  $\mathcal{I}$ . If  $\mathcal{P}$  and  $Q$  have no boundary, i.e., every edge is glued to another edge, then so will  $\mathcal{I}$ . (In fact, we can achieve this property of  $\mathcal{I}$  more generally by gluing together boundary edges of  $\mathcal{I}$  of equal length.)

**Cut 2:** For each triangle  $\triangle AEI$ , cut the outer edges  $AB$ ,  $DE$ ,  $EF$ ,  $HI$ ,  $IJ$ , and  $LA$  (represented by purple dashed lines in Figure 9). Because no cut fully separates an entire edge from its mate in  $Q$ , this cutting preserves connectivity. (If we glued together boundary edges during the previous step, Glue 1, cut those edges also.)

**Glue 2:** For each triangle  $\triangle AEI$ , glue the outer edges  $AB$ ,  $DE$ ,  $EF$ ,  $HI$ ,  $IJ$ , and  $LA$  to their neighbors in  $Q$  when they exist (as in Figure 9, right). Now every edge is fully glued as in  $Q$ , so we have arrived at manifold  $Q$ .

## 5.2 Embeddable Intermediate Polyhedron via Burago–Zalgaller Theorem

The above construction of an abstract intermediate manifold  $\mathcal{I}$  is actually already guaranteed to be embeddable in 3D whenever the input manifolds  $\mathcal{P}$  and  $Q$  are so embedded. Because  $\mathcal{P}$  and  $Q$  are embedded, they either are both orientable or both have boundary. Our construction for  $\mathcal{I}$  inherits either property. Then we can apply a powerful result of Burago and Zalgaller:

**Theorem 10** ([BZ96, Theorem 1.7]). *Every polyhedral manifold that is either orientable or has boundary admits an isometric piecewise-linear  $C^0$  embedding into 3D.*

Unfortunately, this embedding is quite complicated. See [Sau12] for a description. Thus we develop an alternative solution that involves modifying the 2-step refolding and intermediate manifold.

## 5.3 Explicit Embeddable Intermediate Polyhedron

Next we describe the modifications necessary to make the intermediate manifold  $\mathcal{I}$  relatively easy to embed in 3D, assuming that the input manifolds  $\mathcal{P}$  and  $Q$  are so embedded. The main idea is to cut each triangle further so that the area next to each edge can unravel into a long doubly covered “strip” that lets it reach far away to its neighbor in the other manifold. To enable a particularly clean construction (shown in Figure 10), we need to guarantee that most triangles are acute.

In more detail, our construction of the intermediate manifold  $\mathcal{I}$  works as follows:

1. First we construct a common *nonobtuse* triangulation of manifolds  $\mathcal{P}$  and  $Q$ , by taking the common dissection described in Section 5.1 and subdividing according to the method of Saraf [Sar09]. In the language of [Sar09, Theorem 2.3], we are given a “subdivided polyhedral surface” (the common dissection), and we want to “subtriangulate” the polygons into nonobtuse triangles that fit together into a proper triangulation of the entire surface (where triangles meet at whole edges, never partial edges). This algorithm has two additional properties that we exploit:
  - (a) The algorithm subdivides the edges of the input polygons, and then triangulates the interior of each input polygon without introducing any more vertices on the edges. The subdivision of each edge depends only on the length of the edge and global parameters (the minimum angle and the minimum edge length in the input polygons). In particular,

the subdivision and triangulation depends on the geometry of the input polygons, but not on the combinatorial information of which faces are glued together. Thus, the subdivision and triangulation will be the same when applied to both  $\mathcal{P}$  and  $\mathcal{Q}$ , so we obtain a common nonobtuse triangulation.

- (b) The algorithm to triangulate each input polygon first builds a layer of triangles around the boundary, based on properties of the edge subdivision algorithm, and then fills in the remaining interior with nonobtuse triangles (mostly by starting with a nearly square rectangular grid). This algorithm guarantees that the triangles sharing an edge with the boundary of the input polygon are all strictly acute. Thus we can assume that all right triangles in the common triangulation have the same neighboring triangles in both  $\mathcal{P}$  and  $\mathcal{Q}$ ; only acute triangles have differing neighbors between  $\mathcal{P}$  and  $\mathcal{Q}$ .

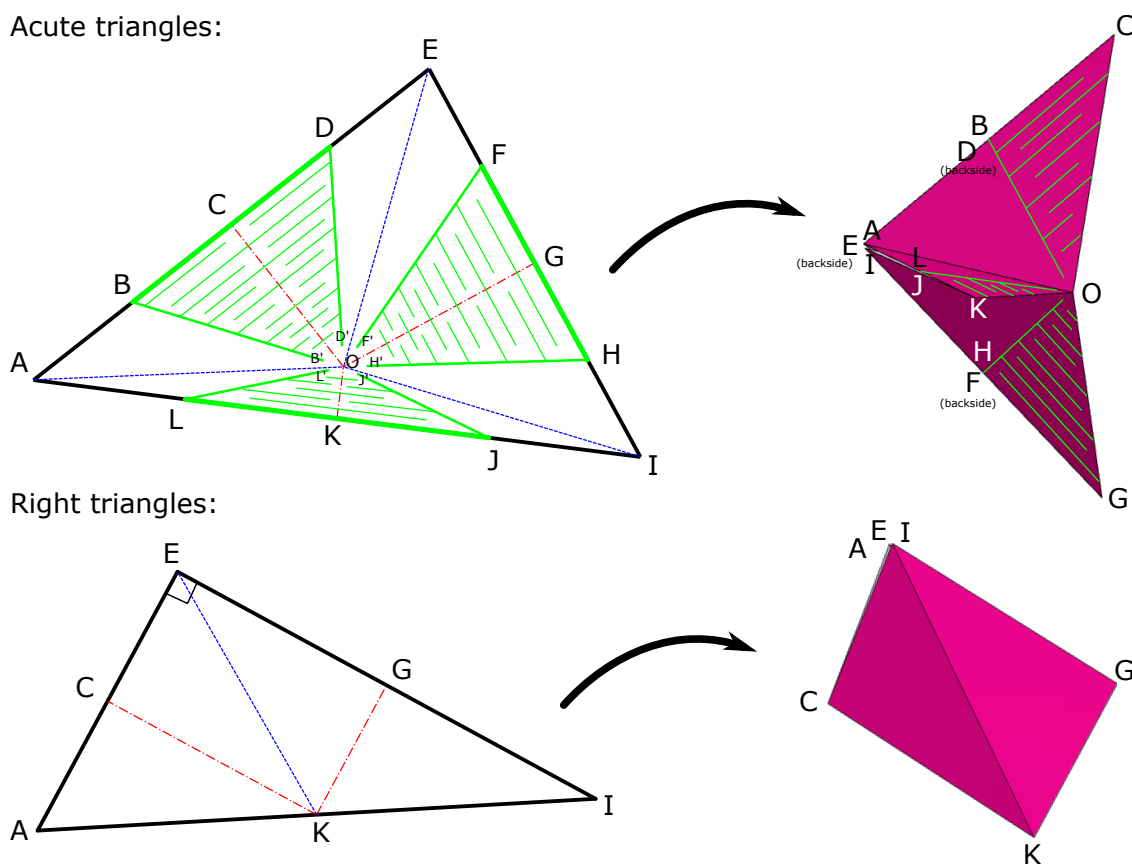


Figure 10: Acute and right triangles crease/cut patterns (left) and resulting 3D structure after folding (right).

- For every triangle in the common triangulation as viewed on  $\mathcal{P}$ , we collapse the triangle according to a crease pattern drawn in Figure 10. Here,  $X'$  is a point on  $XO$  very close to  $O$ . For an acute triangle  $\triangle AEI$  (Figure 10, top left), we mountain fold the perpendicular bisectors  $OC$ ,  $OG$ , and  $OK$  by  $180^\circ$ , which meet at the circumcenter  $O$ , and valley fold the lines  $OA$ ,  $OE$ , and  $OI$  connecting  $O$  to the triangle vertices, each by  $60^\circ$ . Then we can collapse the structure into a 3D rabbit-ear-like doubly covered structure shown in Figure 10 (top right). For a right triangle  $\triangle AEI$  (Figure 10, bottom left), the circumcenter  $O$  lands on the midpoint  $K$  of the hypotenuse, and we need only three folds: two mountain folds on the perpendicular

bisectors  $CK$  and  $GK$  on the sides adjacent to the right angle, and a valley fold from the circumcenter  $O = K$  to the right-angle vertex.

3. For every acute triangle in the common triangulation as viewed on  $\mathcal{P}$ , we cut along the pattern of green lines drawn in the top row of Figure 10. In the 3D rabbit-ear-like doubly covered folding, these cuts make a zig-zag strip out of the material near the middle half of each edge, enabling the material to fold far away while remaining doubly covered. Because of the double covering, we can glue the cuts together between the two layers, so that we do not introduce any boundary in manifold  $\mathcal{I}$ .
4. Similar to the abstract manifold from Section 5.1, we cut along the inner edges  $BC, CD, FG, GH, JK,$  and  $KL$ , and then glue them to their neighbors in  $\mathcal{Q}$ . But now the green cuts allow for this connection to be stretched around the rest of the manifold to avoid collisions (as detailed below).
5. To reduce the number of connections from  $\mathcal{P}$  that we need to preserve, we also cut along many of the outer edges  $AB, DE, EF, HI, IJ,$  and  $LA$  of the triangles  $\triangle AEI$ . Specifically, we construct a spanning tree on the dual graph of the common triangulation as viewed on  $\mathcal{P}$ , and then cut all outer edges between triangles that are not adjacent in the spanning tree. Then we glue these edges to each other locally within their triangle ( $AB$  to  $DE, EF$  to  $HI,$  and  $IJ$  to  $LA$ ), so that we do not introduce any boundary in manifold  $\mathcal{I}$ .

Although we described the construction of  $\mathcal{I}$  in terms of multiple cut and glue steps, it is in fact formed by performing all cut steps followed by all glue steps, as detailed below. The cut steps preserve connectivity because of the spanning tree of the dual graph of the common triangulation viewed on  $\mathcal{P}$ .

**Lemma 11.** *The manifold  $\mathcal{I}$  constructed above can be embedded in 3D (in fact, **flat folded** into a stack of 2D layers) with zero volume.*

*Proof.* To construct the embedding of  $\mathcal{I}$ , we first show how to combine the rabbit-ear-like doubly covered folding of each triangle from Figure 10 into a single structure that achieves all connections in  $\mathcal{P}$ . Refer to Figure 11.

1. As shown in Figure 11a, we start with the common nonobtuse triangulation as viewed on  $\mathcal{P}$ , draw all the perpendicular bisector folds (blue lines) which also act as the dual graph, and cut all but a spanning tree of this dual graph (red lines). We also choose a leaf in the spanning tree (highlighted red) to serve as the root of the tree, so that every node has at most two children.
2. As shown in Figure 11b, we fold each triangle into the rabbit-ear-like doubly covered structure from Figure 10, but flattened into the plane. Now we see how connections between neighboring triangles work: the foldings share the folded-in-half common edge  $CFB$  and live on opposite sides of that line. Figure 11c shows a zoomed-in view of two adjacent folded triangles.
3. Figure 11d shows a parent triangle and its up to two children triangles. We recursively construct an embedding of each child rooted subtree, and then combine them by keeping the layers of each child subtree completely above or below the layers of the other child subtree as well as the parent triangle. Thus we obtain an embedding of the parent's rooted subtree. In the end, all vertices of the triangles collapse down to a single central point  $C$ , and all circumcenters  $O_i$  will be scattered around  $C$  and connected to  $C$  via an edge.

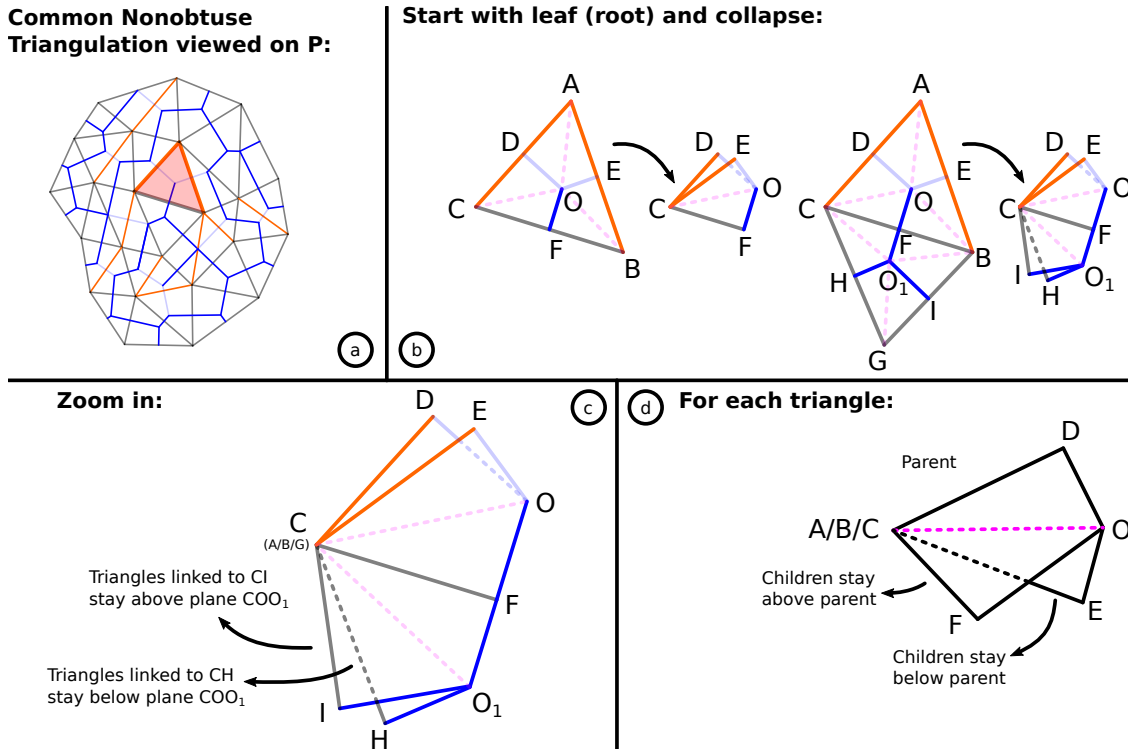


Figure 11: Flat folding the intermediate manifold  $\mathcal{I}$  without self-intersection. We do not attempt to represent the zig-zag strips and their folding.

Next we extend the zig-zag arms of the triangles to reach their neighbors in  $\mathcal{Q}$ . These arms end at the edges  $CO_i$ . By folding the zig-zag arms into a long straight strip, we can extend the arms arbitrarily far (by adding appropriately many zig-zags). By extending the arms sufficiently far, they can exit the folded tree structure described above. Then we can navigate the arms to meet each other according to the edge pairing in the common triangulation as viewed on  $\mathcal{Q}$ . Although ugly, this is possible without self-intersection and without adding any boundary.  $\square$

Our 2-step refolding algorithm from  $\mathcal{P}$  to  $\mathcal{I}$  to  $\mathcal{Q}$  works as follows:

**Cut 1:**

- Cut manifold  $\mathcal{P}$  along all edges except a spanning tree of the dual graph of the common nonobtuse triangulation as viewed on  $\mathcal{P}$ . These cuts preserve connectivity by the spanning-tree property.
- For every acute triangle in the common triangulation, cut the green lines drawn in Figure 10 (left). Because no edge gets fully cut and no cut divides a face in two, connectivity is preserved.

**Glue 1:** For each triangle  $\triangle AEI$ :

- For each green zig-zag edge in Figure 10, glue it to its reflection across the mountain line of symmetry, forming a doubly covered zig-zag strip. In particular, glue the boundaries:  $BB'$  to  $DD'$ ,  $FF'$  to  $HH'$ ,  $JJ'$  to  $LL'$ .

- If the following edges are not already attached via the spanning tree, glue  $AB$  to  $ED$ ,  $EF$  to  $IH$ , and  $IJ$  to  $AL$ .
- Glue the inner edges  $BC, CD, FG, GH, JK$ , and  $KL$  across to corresponding edges of the neighboring triangle in  $\mathcal{Q}$ .

The second cut and glue steps are similar to the abstract construction in Section 5.1:

**Cut 2:** For each triangle  $\triangle AEI$ :

- Cut the outer edges  $AB, DE, EF, HI, IJ$ , and  $LA$ .
- Cut the green edges, including the boundaries  $BB', DD', FF', HH', JJ'$ , and  $LL'$ .

**Glue 2:** For each triangle  $\triangle AEI$ :

- Glue the outer edges  $AB, DE, EF, HI, IJ$ , and  $LA$  to their neighbors in  $\mathcal{Q}$  when they exist.
- Glue the green edges back together to form the triangle on the left of Figure 10.

We arrive at manifold  $\mathcal{Q}$ .

## 5.4 Full Example

In this section, we demonstrate our 2-step refolding algorithm with a simple nontrivial example, shown in Figure 12: a triangular bipyramid  $\mathcal{P}$  to flat hexagon  $\mathcal{Q}$ .

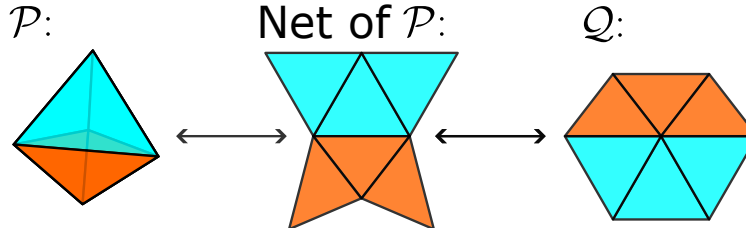


Figure 12: Goal for the example: transform the triangular bipyramid  $\mathcal{P}$  into the flat hexagon  $\mathcal{Q}$ .

Figure 13 shows the intermediate manifold  $\mathcal{I}$  for these  $\mathcal{P}$  and  $\mathcal{Q}$ . In both the flat unfolding on the left and the folded form on the right, we can see the gluings for both  $\mathcal{P}$  and  $\mathcal{Q}$  via solid and dashed lines respectively.

Figure 14 shows photographs of a physical execution of this refolding. The refolding steps are as follows:

**Cut 1:** Starting with  $\mathcal{P}$  in Figure 14a, we edge-unfold  $\mathcal{P}$  into an unfolding (Figure 14b). Then we further fold and cut each individual triangle in accordance with Figure 10 to obtain Figure 14c. For the purposes of this demonstration, however, we cut only the necessary zig-zags into the physical paper.

**Glue 1:** Next we glue the zig-zag strips to their target location as defined on  $\mathcal{Q}$  to obtain  $\mathcal{I}$ , as shown in Figure 14d.

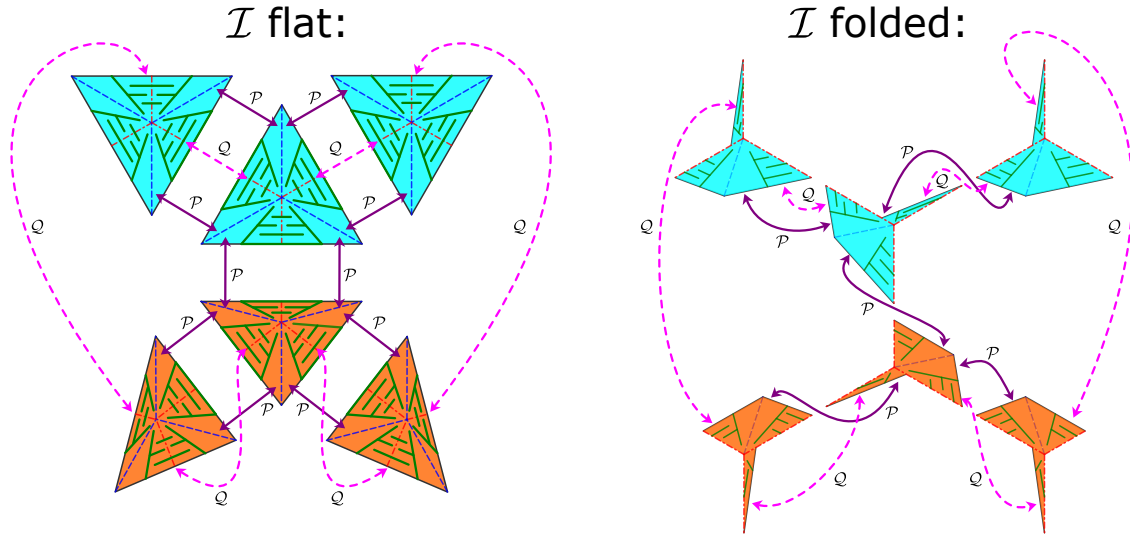


Figure 13: Illustration of the intermediate manifold  $\mathcal{I}$  in its flat state (left) and folded state (right), with folds and cuts for each triangle in accordance with Figure 10.

**Cut 2:** To transform from  $\mathcal{I}$  to  $\mathcal{Q}$ , we first cut all the connections from  $\mathcal{P}$  in  $\mathcal{I}$ , which allows for the shape to be re-arranged into something close to the target manifold  $\mathcal{Q}$  (Figure 14e). Then we cut the previously glued together zig-zag edges. The result can flatten out to the full manifold  $\mathcal{Q}$ , as shown in Figure 14f.

**Glue 2:** Finally, glue all the matching edges together to form  $\mathcal{Q}$ .

## 5.5 Transformation Between $n$ Polyhedral Manifolds

In this section, we extend our techniques to prove Corollary 9: 2-step refolding between  $n$  polyhedral manifolds  $\mathcal{P}_1, \mathcal{P}_2, \dots, \mathcal{P}_n$  via the same intermediate manifold  $\mathcal{I}$ .

Figure 15 illustrates the abstract case. Instead of dividing each edge into four equal segments, we divide them into  $2n$  equal segments, where the  $i$ th successive nested pair of segments attach to the triangle's neighbor in  $\mathcal{P}_i$ . Then we apply similar constructions to Section 5.3 for each acute triangle, as follows:

1. Find the circumcenter and fold into a rabbit-ear-like doubly covered structure, just as in Figure 10.
2. Cut the zig-zag pattern shown in Figure 10 for each pair of  $\mathcal{P}_i$  edges on each edge of the triangle, for  $i > 1$ . (For  $\mathcal{P}_1$ , we can avoid these cuts, like  $\mathcal{P}$  in Figure 10.)
3. Extend each zig-zag strip to attach to its neighbor in  $\mathcal{P}_i$ .

To transform from this intermediate manifold  $\mathcal{I}$  to any target  $\mathcal{P}_i$ , we cut all connections except for the  $\mathcal{P}_i$  connections, and glue all cut edges according to  $\mathcal{P}_i$ .

## 6 Conclusion

In this paper, we showed a transformation algorithm between any two manifolds with two cut-and-glue refolding steps. When transforming between manifold  $\mathcal{P}$  and manifold  $\mathcal{Q}$ , we go through

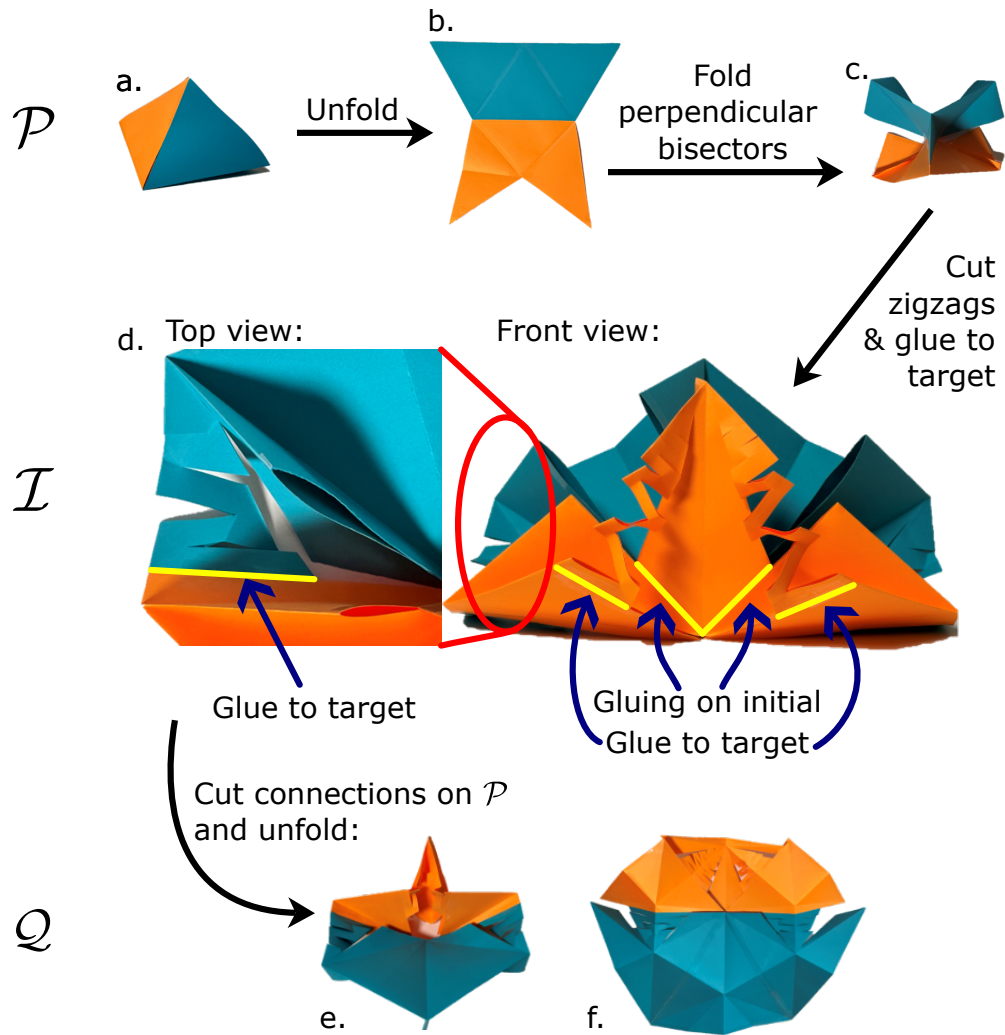


Figure 14: Physical example of transformation shown in Figure 12

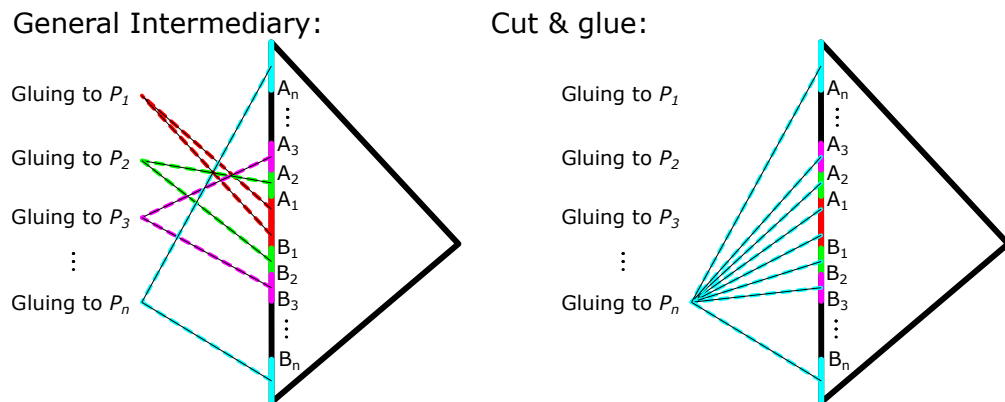


Figure 15: Intermediate manifold  $\mathcal{I}$  for 2-step folding between  $n$  polyhedral manifolds  $\mathcal{P}_1, \mathcal{P}_2, \dots, \mathcal{P}_n$ , and the cut-and-glue step to transform to manifold  $\mathcal{P}_n$ .



an intermediate embeddable polyhedron which is not necessarily convex. We also showed two simpler refolding algorithms for doubly covered polyhedra and tree-shaped polycubes.

Many open questions remain:

- Are there examples where 1-step refolding is impossible?
- If the two given polyhedra are convex, is there a finite-step refolding where the intermediate polyhedra are also convex? [DO07, Section 25.8.3]
- Can we extend our polycube result to avoid self-intersection without well-separation, or to support non-tree-shaped polycubes of the same surface area?
- Can we improve the number of refolding steps needed for the doubly covered polygon or polycube refolding algorithms?

## References

- [AAC<sup>+</sup>12] Timothy G. Abbott, Zachary Abel, David Charlton, Erik D. Demaine, Martin L. Demaine, and Scott Duke Kominers. Hinged dissections exist. *Discrete & Computational Geometry*, 47(1):150–186, 2012.
- [AAK<sup>+</sup>24] Zachary Abel, Hugo A. Akitaya, Scott Duke Kominers, Matias Korman, and Frederick Stock. A universal in-place reconfiguration algorithm for sliding cube-shaped robots in a quadratic number of moves. In *Proceedings of the 40th International Symposium on Computational Geometry*, pages 1:1–1:14, 2024.
- [ACD<sup>+</sup>08] Greg Aloupis, Sébastien Collette, Erik D. Demaine, Stefan Langerman, Vera Sacristán, and Stefanie Wuhrer. Reconfiguration of cube-style modular robots using  $O(\log n)$  parallel moves. In *Proceedings of the 19th Annual International Symposium on Algorithms and Computation (ISAAC 2008)*, pages 342–353, Gold Coast, Australia, December 2008.
- [ACD<sup>+</sup>09] Greg Aloupis, Sébastien Collette, Mirela Damian, Erik D. Demaine, Robin Flatland, Stefan Langerman, Joseph O’Rourke, Suneeta Ramaswami, Vera Sacristán, and Stefanie Wuhrer. Linear reconfiguration of cube-style modular robots. *Computational Geometry: Theory and Applications*, 42(6–7):652–663, August 2009.
- [ADKU22] Elena Arseneva, Erik D. Demaine, Tonan Kamata, and Ryuhei Uehara. Discretization to prove the nonexistence of “small” common unfoldings between polyhedra. In *Proceedings of the 34th Canadian Conference on Computational Geometry (CCCG 2022)*, Toronto, Ontario, Canada, August 25–27 2022.
- [Bol33] Farkas Bolyai. *Tentamen juventutem studiosam in elementa matheseos purae, elementaris ac sublimioris, methodo intuitiva, evidentiaque huic propria, introducendi*. Typis Collegii Refomatorum per Josephum et Simeonem Kali, Maros Vásárhely, 1832–1833.
- [BZ96] Yu. D. Burago and V. A. Zalgaller. Isometric piecewise linear immersions of two-dimensional manifolds with polyhedral metrics into  $\mathbb{R}^3$ . *St. Petersburg Mathematical Journal*, 7(3):369–385, 1996.
- [DDD<sup>+</sup>23] Erik D. Demaine, Martin L. Demaine, Jenny Diomidova, Tonan Kamata, Ryuhei Uehara, and Hanyu Alice Zhang. Any Platonic solid can transform to another by  $O(1)$  refoldings. *Computational Geometry: Theory and Applications*, 113:101995, 2023.

- [DO07] Erik D. Demaine and Joseph O'Rourke. *Geometric Folding Algorithms: Linkages, Origami, Polyhedra*. Cambridge University Press, July 2007.
- [Ger33] Paul Gerwien. Zerschneidung jeder beliebigen Anzahl von gleichen geradlinigen Figuren in dieselben Stücke. *Journal für die reine und angewandte Mathematik (Crelle's Journal)*, 10:228–234 and Taf. III, 1833.
- [Low14] Mr. Lowry. Solution to question 269, [proposed] by Mr. W. Wallace. In T. Leybourn, editor, *Mathematical Repository*, volume 3, part 1, pages 44–46. W. Glendinning, London, 1814.
- [Sar09] Shubhangi Saraf. Acute and nonobtuse triangulations of polyhedral surfaces. *European Journal of Combinatorics*, 30(4):833–840, 2009.
- [Sau12] Emil Saucan. Isometric embeddings in imaging and vision: Facts and fiction. *Journal of Mathematical Imaging and Vision*, 43(2):143–155, June 2012.
- [Wal31] William Wallace. *Elements of Geometry*. Bell & Bradfute, Edinburgh, 8th edition, 1831.